DE GRUYTER
OPEN

Arch. Min. Sci. **62** (2017), 4, 753-774

Electronic version (in color) of this paper is available: http://mining.archives.pl

DOI 10.1515/amsc-2017-0053

M. ABDIA*, H. MOLLADAVOODI*#, H. SALARIRAD*

ROCK FAILURE ANALYSIS BASED ON A COUPLED ELASTOPLASTIC-LOGARITHMIC DAMAGE MODEL

MODEL PĘKANIA SKAŁ OPARTY NA SPRZĘŻONYM ELASTOPLASTYCZNO-LOGARYTMICZNYM MODELU USZKODZEŃ

The rock materials surrounding the underground excavations typically demonstrate nonlinear mechanical response and irreversible behavior in particular under high in-situ stress states. The dominant causes of irreversible behavior are plastic flow and damage process. The plastic flow is controlled by the presence of local shear stresses which cause the frictional sliding. During this process, the net number of bonds remains unchanged practically. The overall macroscopic consequence of plastic flow is that the elastic properties (e.g. the stiffness of the material) are insensitive to this type of irreversible change. The main cause of irreversible changes in quasi-brittle materials such as rock is the damage process occurring within the material. From a microscopic viewpoint, damage initiates with the nucleation and growth of microcracks. When the microcracks length reaches a critical value, the coalescence of them occurs and finally, the localized meso-cracks appear. The macroscopic and phenomenological consequence of damage process is stiffness degradation, dilatation and softening response.

In this paper, a coupled elastoplastic-logarithmic damage model was used to simulate the irreversible deformations and stiffness degradation of rock materials under loading. In this model, damage evolution & plastic flow rules were formulated in the framework of irreversible thermodynamics principles. To take into account the stiffness degradation and softening on post-peak region, logarithmic damage variable was implemented. Also, a plastic model with Drucker-Prager yield function was used to model plastic strains.

Then, an algorithm was proposed to calculate the numerical steps based on the proposed coupled plastic and damage constitutive model. The developed model has been programmed in VC++ environment. Then, it was used as a separate and new constitutive model in DEM code (UDEC). Finally, the experimental Oolitic limestone rock behavior was simulated based on the developed model. The irreversible strains, softening and stiffness degradation were reproduced in the numerical results. Furthermore, the confinement pressure dependency of rock behavior was simulated in according to experimental observations.

Keywords: Damage mechanics, Plasticity, Stiffness degradation, Logarithmic damage variable, Brittleness parameter

* AMIRKABIR UNIVERSITY OF TECHNOLOGY,DEPARTMENT OF MINING AND METALLURGICAL ENGINEERING, TEHRAN, IRAN

Corresponding author: hamedavodi@aut.ac.ir

Zachowanie materiału skalnego otaczającego wyrobiska podziemne w odpowiedzi na wysokie stany lokalnych naprężeń działajacych in situ jest zazwyczaj nieodwracalne i nieliniowe. Reakcje nieodwracalne spowodowane są w głównej mierze przez płynięcie plastyczne i procesy uszkodzeń. Płynięcie plastyczne uwarunkowane jest przez występowanie lokalnych naprężeń ścinających powodujące obsunięcia skał. W trakcie tego procesu ilość wiązań netto pozostaje praktycznie niezmieniona. Całościowy efekt płynięcia plastycznego w skali makroskopowej polega na tym, że właściwości elastyczne (np. sztywność) stają się niewrażliwe na działanie nieodwracalnych procesów tego rodzaju. Podstawową przyczyną reakcji nieodwracalnych reakcji w materiałach quasi-kruchych, do których należą skały, jest powstawanie uszkodzeń wewnątrz materiału. W skali mikroskopowej, proces uszkodzenia rozpoczyna się od zainicjowania i stopniowej propagacji mikro- pęknięć. Gdy długość mikro- pęknięć osiągnie wartość graniczną, zaczynają one łączyć się ze sobą w rezultacie powodując powstanie lokalnych mezo- pęknięć. W ujeciu makroskopowym i fenomenologicznym, następstwami procesu uszkodzenia jest obniżenie sztywności, powstawanie dylatacji szczelin oraz miękniecie materiału.

W pary wykorzystano sprzężony model elastoplastyczno- logarytmiczny do symulacji nieodwracalnych odkształceń i utraty sztywności materiału skalnego pod wpływem naprężeń. W modelu tym ewolucje uszkodzeń i opis płynięcia plastycznego sformułowano w oparciu o reguły nieodwracalnych przemian termodynamicznych. Aby uwzględnić utratę sztywności oraz miękniecie materiału w obszarach gdzie występowały największe naprężenia wykorzystano zmienną logarytmiczną opisującą uszkodzenie. Odkształcenia plastyczne zamodelowano z wykorzystaniem modelu plastycznego opartego na warunku plastyczności Drukera- Pragera.

Zaproponowano także algorytm do obliczania kolejnych kroków procedury numerycznej, oparty na zaproponowanym modelu plastycznym oraz konstytutywnym modelu uszkodzeń. Opracowany model pracuje w środowisku VC++. Został on następnie wykorzystany jako osobny, nowy model konstytutywny zapisany w kodzie DEM (UDEC). W części końcowej przeprowadzono symulację zachowania wapienia oolitowego w oparciu o zaproponowany model. Nieodwracalne odkształcenia, utrata sztywności zostały odtworzone w postaci wyników procedury numerycznej. Ponadto, przeprowadzono symulacje zachowania skał w zależności od działającego na nie ciśnienia w oparciu o obserwacje eksperymentalne.

Słowa kluczowe: wytrzymałość materiału na uszkodzenia, plastyczność, utrata sztywności, zmienna logarytmiczna opisująca uszkodzenie, kruchość

Nomenclature

α – Drucker-Pruger friction parameter
β – Drucker-Pruger dilation parameter
C – Drucker-Pruger cohesion parameter
d – scalar damage variable
ε_{ij} – total strain tensor
$\dot{\varepsilon}_{ij}$ – increment of total strain tensor
ε^{e}_{ij} – elastic part of strain tensor
ε^{p}_{ij} – plastic part of strain tensor
ε_c – strain corresponding to uniaxial compressive strength
E^{0}_{ijkl} – undamaged fourth order elastic stiffness tensor
E_{ijkl} – fourth order elastic stiffness tensor of damaged material
$E^{t^{ed}}_{ijkl}$ – tangent elastic stiffness tensor in the elastic-damage condition
$E^{t^{ep}}_{ijkl}$ – tangent elastic stiffness tensor in the elastic-plastic condition
f_c – uniaxial compressive strength
f_t – uniaxial tensile strength

F^L – logarithmic damage criterion
F^d – scalar damage criterion
F^p – plastic yield function
g_f – fracture energy per unit volume
J_2' – second invariant of the deviatoric stress tensor
K – brittleness parameter
L – logarithmic damage variable
$\dot{L}$ – logarithmic damage multiplier
Q^p – plastic potential function
σ_{ij} – stress tensor
$\dot{\sigma}_{ij}$ – increment of stress tensor
σc – uniaxial compressive strength
σ_{kk} – first invariant of the normal stress tensor
$r(d)$ – resistance functions corresponding to scalar damage variable
$r(L)$ – resistance functions corresponding to logarithmic damage variable
r_0 – modulus of resilience
s_{ij} – deviatoric stress tensor
ψ – free energy thermodynamic potential function
ψ^p – plastic part of free energy thermodynamic potential function
$\dot{\lambda}^p$ – plastic multiplier
Y_d – thermodynamic force associated with the scalar damage variable
Y_L – thermodynamic force associated with the logarithmic damage variable

1. Introduction

Due to increasing human needs to rock excavations, the analysis of stress and strain surrounding rock mass and stability evaluation of these excavations are essential. Rocks surrounding excavations under induced stresses have non elastic, nonlinear mechanical behavior within the elastic stiffness degradation and unrecoverable plastic strains. In this regard, the inelasticity associated with most of the brittle solids, during external loadings, is the result of two kinds of irreversible changes: microcracking (damage process) and frictional sliding along microcracks. These two kinds of irreversible phenomena, which may be assumed to occur in coupled or uncoupled forms, lead to the degradation of elastic property of the material and the development of moderate to large permanent deformations at the macro-scale level, respectively.

The strain softening and elastic stiffness degradation on macro-scale are due to the damage process including nucleation, growth and propagation of microcracks on micro-scale of rocks, while the plastic strains are due to the frictional sliding along microcracks faces. The most of experimental observations in the past few years have shown that the use of plasticity theories is appropriate to model the deformation component caused by frictional sliding along microcracks, whereas the use of damage mechanics theories to model the nucleation and propagation of microcracks is clearly evident in the literature. Therefore, these two mechanisms –microcracking and frictional sliding – are to be addressed properly through the use of combined damage and plasticity theories, while developing constitutive models for brittle solids. Many researchers (Addessi et al., 2002; Bazant & Kim, 1979; Dragon & Mrotz, 1979; Hansen et al., 2001; Jefferson, 2003;

Ortiz & Popov, 1982; Ortiz, 1985; Salari et al., 2005; Simo & Ju, 1987; Voyiadjis et al., 2008; Yazdani & Karnawat, 1996; Yazdani & Schreyer, 1990; Shao et al., 2006; Chiarellia et al., 2003; Kamal et al., 2013; Wang et al., 2016; Li et al., 2014) have adopted combined damage-plasticity approach in the constitutive modeling of brittle solids such as concrete and rocks .

Furthermore, using of logarithmic damage model proposed by Carol et al. (2001), the elastic stiffness degradation and strain softening on post-peak region can be considered simultaneously. The damage law was formulated in terms of the so-called logarithmic damage variable and its associated thermodynamic force, which is physically meaningful and corresponds to the density of energy stored in the deformation of the damaged material. In this regard, to simulate of rock behavior, the logarithmic damage model has been implemented in the laboratory and field scales data (Molladavoodi & Mortazavi, 2011; Mortazavi & Molladavoodi, 2012). Although the coupled elastoplastic-damage model has been proposed in literature to simulate the pre-peak behavior, in this investigation, to take into account the elastic stiffness degradation, strain softening and irreversible strains at the same time especially on post-peak region, the coupled elastoplastic-logarithmic damage model has been proposed.

Despite the fact that some micromechanical damage models based on homogenization procedure have been proposed recently to take into account sliding and damage mechanisms of microcracks (Zhu et al., 2008,2011; Molladavoodi, 2015), in this investigation a phenomenological logarithmic damage model coupled with plasticity has been applied for the sake of its simplicity in analysis of the complex behavior of rocks especially on post-peak region.

The proposed coupled elastoplastic-logarithmic damage model has been formulated in the framework of continuum thermodynamics using of the internal variables. In this regard, a Drucker-Prager yield function has been applied for plastic loading of the material and a non-associated flow rule has been employed to control inelastic dilatancy. Hence, the formulation and computational procedure of the proposed model have been presented in this paper.

Although, the plastic models have usually been implemented in geomechanics numerical software in order to non-linear analysis of rock excavations, to take into account the damage process and plastic flow simultaneously, the combined implementation of damage mechanics and plasticity is essential. In this study, the proposed coupled elastoplastic-logarithmic damage model has been programmed and implemented into a commercial software to simulate the Oolithic limestone rock, finally, a number of load histories are examined to investigate the performance of the model.

2. The principles of the proposed model

In this paper, based on experimental investigations, a coupled elastoplastic-logarithmic damage model has been proposed for the description of mechanical behavior of rock materials. As classically, assuming the isothermal conditions and infinitesimal strains, the total strain tensor is decomposed into an elastic part (ε_{ij}^{e}) and plastic part (ε_{ij}^{p}) (Shao et al., 2006):

$$\varepsilon_{ij} = \varepsilon_{ij}^{e} + \varepsilon_{ij}^{p}\,,\ \dot{\varepsilon}_{ij} = \dot{\varepsilon}_{ij}^{e} + \dot{\varepsilon}_{ij}^{p} \tag{1}$$

For this class of materials, an isotropic damage can be used to introduce the macro-scale effect of microcracks existence in micro-scale. In a representative volume element (RVE) with randomly distributed microcracks, the isotropic and scalar damage variable (d) is defined in

a phenomenological way by the surface density of microcracks lying on a plane cutting the RVE (Lemaitre & Desmorat, 2005). The scalar damage variable varies from zero corresponding to undamaged state to one representing the damaged status. With applying a logarithmic change of the damage variable, the logarithmic damage variable (L) can be defined as below (Carol et al., 2001):

$$L = ln\left(\frac{1}{1-d}\right),\ d = 1 - e^{-L} \tag{2}$$

In the scalar damage variable case, the fourth order elastic stiffness tensor of damaged material (E_{ijkl}) can be written as

$$E_{ijkl} = \left(1-d\right) E^{0}_{ijkl}\ 0 \le d \le 1 \tag{3}$$

While E^{0}_{ijkl} is the undamaged fourth order elastic stiffness tensor (without microcracks). Nevertheless, in the logarithmic damage variable case, the fourth order elastic stiffness tensor of damaged material can be written as

$$E_{ijkl} = e^{-L} E^{0}_{ijkl}\ 0 \le L \le \infty \tag{4}$$

With postulation the coupling of damage process and plasticity, the free energy thermodynamic potential function can be expressed by (Conil et al., 2004):

$$\psi = \frac{1}{2}\left(\varepsilon_{ij} - \varepsilon^{p}_{ij}\right) E_{ijkl}\left(\varepsilon_{kl} - \varepsilon^{p}_{kl}\right) + \psi^{p}\left(\gamma_{p}\right) \tag{5}$$

While γ_p and ψ^p are the plastic hardening internal variable and the locked plastic hardening energy respectively. Finally, the state equation for stress tensor was obtained by derivative of the free energy thermodynamic potential function with respect to the elastic strain tensor (Rashid et al., 2003).

$$\sigma_{ij} = \frac{\partial \psi}{\partial \varepsilon^{e}_{ij}} = E_{ijkl}\left(\varepsilon_{kl} - \varepsilon^{p}_{kl}\right) = E_{ijkl}\,\varepsilon^{e}_{kl} \tag{6}$$

On the basis of equation (6), the stress tensor increment ($\dot{\sigma}_{ij}$) can be calculated as below

$$\dot{\sigma}_{ij} = E_{ijkl}\,\dot{\varepsilon}^{e}_{kl} + \dot{E}_{ijkl}\,\varepsilon^{e}_{kl} \tag{7}$$

Therefore, a damage evolution and plastic flow rule must be determined to compute the stress tensor increment in equation (7). In this regard, to compute the increment of elastic stiffness tensor ($\dot{E}_{ijkl}$), the derivative of elastic stiffness tensor with respect to logarithmic damage variable is multiplied by the logarithmic damage variable increment ($\dot{L}$) as below

$$\dot{E}_{ijkl} = \frac{\partial E_{ijkl}}{\partial L}\dot{L} = -e^{-L} E^{0}_{ijkl}\,\dot{L} = -E_{ijkl}\dot{L} \tag{8}$$

By substitution the equation (8) into (7), we have

$$\dot{\sigma}_{ij} = E_{ijkl}\,\dot{\varepsilon}^{e}_{kl} - E_{ijkl}\,\varepsilon^{e}_{kl}\,\dot{L} \tag{9}$$

The thermodynamic force associated with the scalar damage variable (Y_d) representing the energy release rate as a result of the microcracks growth in rock is given by

$$Y_d = -\frac{\partial \psi}{\partial d} = -\frac{1}{2}\left(\varepsilon_{ij} - \varepsilon_{ij}^p\right)\frac{\partial E_{ijkl}}{\partial d}\left(\varepsilon_{kl} - \varepsilon_{kl}^p\right) = \frac{1}{2}\left(\varepsilon_{ij} - \varepsilon_{ij}^p\right)E_{ijkl}^0\left(\varepsilon_{kl} - \varepsilon_{kl}^p\right) \tag{10}$$

In the logarithmic damage variable case, the thermodynamic force associated with the logarithmic damage variable (Y_L) can be calculated as below

$$Y_L = -\frac{\partial \psi}{\partial L} = -\frac{1}{2}\left(\varepsilon_{ij} - \varepsilon_{ij}^p\right)\frac{\partial E_{ijkl}}{\partial L}\left(\varepsilon_{kl} - \varepsilon_{kl}^p\right) = \frac{1}{2}\left(\varepsilon_{ij} - \varepsilon_{ij}^p\right)E_{ijkl}\left(\varepsilon_{kl} - \varepsilon_{kl}^p\right) \tag{11}$$

The physical meaning of the thermodynamic force associated with the logarithmic damage variable is the current strain energy of rock. According to equation (11), the derivative of the thermodynamic force associated with the logarithmic damage variable with respect to the elastic strain tensor and logarithmic damage variable respectively can be calculated as following

$$\frac{\partial Y_L}{\partial \varepsilon_{ij}^e} = E_{ijkl}\left(\varepsilon_{kl} - \varepsilon_{kl}^p\right) = \sigma_{ij}$$

$$\frac{\partial Y_L}{\partial L} = -\frac{1}{2}\left(\varepsilon_{ij} - \varepsilon_{ij}^p\right)E_{ijkl}\left(\varepsilon_{kl} - \varepsilon_{kl}^p\right) \tag{12}$$

2.1. Damage characterization

The damage criterion (F^d) which is the boundary of damage progression in rock is consisting of two principal parts of loading and resistance functions. Therefore, it can be written as (Shao et al., 2006):

$$F^d = f\left(loading\right) - r\left(resist\right) \tag{13}$$

According to equation (13), the loading function is usually expressed as function of the thermodynamic force associated with the damage variable. On the other hand, the resistance function represents the current damage energy release threshold (energy barrier). Therefore, in the scalar damage variable case, the damage criterion is expressed as following:

$$F^d\left(Y_d, d\right) = Y_d - r\left(d\right) \tag{14}$$

In order to consider the strain softening behavior on post-peak region, the resistance function is to be a decreasing power function of the scalar damage variable. Hence it can be written as (Salari et al., 2004):

$$r\left(d\right) = r_0\left(1-d\right)^K,\ K = \frac{r_0}{g_f},\ 0 < K < 1 \tag{15}$$

Here r_0 designates the modulus of resilience, i.e. the elastic strain energy at peak stress in uniaxial strength test as shown in Fig. 1, g_f is the fracture energy per unit volume (area under the complete stress-strain curve) and the exponent K represents the ratio between the modulus of resilience and the fracture energy per volume.

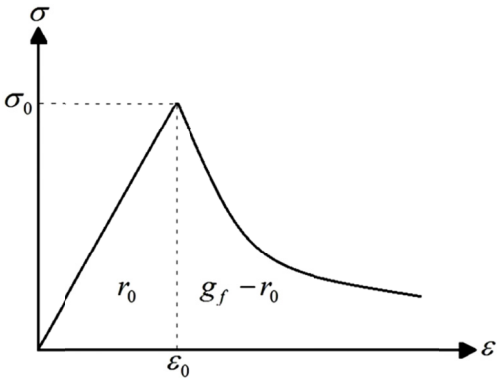

Fig. 1. The complete stress-strain curve in uniaxial strength test (Salari et al., 2004)

Fig. 1 shows the physical meaning of r_0 and g_f parameters clearly. It can be written as:

$$r_0 = \frac{1}{2}\sigma_0\varepsilon_0,\ g_f = \int_0^{\infty}\sigma(\varepsilon).d\varepsilon \tag{16}$$

In the scalar damage variable case, using the equations (10) & (15) the damage criterion can be expressed as following equation:

$$F^d\left(Y_d,d\right) = \frac{1}{2}\left(\varepsilon_{ij}-\varepsilon_{ij}^p\right)E_{ijkl}^0\left(\varepsilon_{kl}-\varepsilon_{kl}^p\right) - r_0\left(1-d\right)^k \tag{17}$$

On the other hand, in the logarithmic damage variable case, by substitution the equation (2) into (15), the resistance function and the damage criterion can be expressed as following

$$r(L) = r_0 e^{-KL} \tag{18}$$

$$F^L\left(Y_L,L\right) = \frac{1}{2}\varepsilon_{ij}^e\, E_{ijkl}\varepsilon_{kl}^e - r_0 e^{-KL} \tag{19}$$

With application of the consistency condition on the above equation ($\dot{F}^L = 0$), we have:

$$\dot{F}^L\left(Y_L,L\right) = \frac{\partial F^L}{\partial Y_L}\left(\frac{\partial Y_L}{\partial \varepsilon_{ij}^e}\dot{\varepsilon}_{ij}^e + \frac{\partial Y_L}{\partial L}\dot{L}\right) - \frac{\partial r(L)}{\partial L}\dot{L} = 0 \tag{20}$$

Using the equations (12) & (20), the increment of logarithmic damage variable under elastic-damage loading condition without plastic flow ($\dot{\varepsilon}_{ij}^p = 0$) can be calculated as following

$$\dot{L} = \frac{\dfrac{\partial Y_L}{\partial \varepsilon_{ij}^e}\dot{\varepsilon}_{ij}}{\left(\dfrac{\partial r(L)}{\partial L} - \dfrac{\partial Y_L}{\partial L}\right)} = \frac{\sigma_{ij}\dot{\varepsilon}_{ij}}{\left(r'(L) + \dfrac{1}{2}\sigma_{kl}\varepsilon_{kl}^e\right)} \tag{21}$$

In which the logarithmic damage multiplier ($\dot{L}$) is a positive scalar expressed from the loading-unloading condition according to the Kuhn-Tucker relations (Shao et al., 2006):

$$F^L\left(Y_L, L\right) = 0, \dot{L} \geq 0,\ F^L\left(Y_L, L\right)\dot{L} = 0 \tag{22}$$

The rate form of the constitutive equation (9) under elastic-damage loading condition without plastic flow ($\dot{\varepsilon}_{ij}^{p} = 0$) becomes:

$$\dot{\sigma}_{ij} = E_{ijkl}^{t^{ed}}\,\dot{\varepsilon}_{kl} \tag{23}$$

In the above equation, $E_{ijkl}^{t^{ed}}$ is the tangent elastic stiffness tensor in the elastic-damage condition. Substitution the increment of logarithmic damage variable obtained in equation (21) into equation (9) without plastic flow, the tangent elastic stiffness tensor is given by

$$E_{ijkl}^{t^{ed}} = E_{ijkl} - \frac{\left(E_{ijqs}\varepsilon_{qs}^{e}\right)\cdot\left(E_{klcd}\varepsilon_{cd}^{e}\right)}{\left(\dfrac{\partial r(L)}{\partial L} - \dfrac{\partial Y_L}{\partial L}\right)} \tag{24}$$

2.2. Plastic characterization

The rock plastic behavior is determined with yield function (F^P), hardening and plastic flow rules. For rock materials, the dilatancy was usually considered by non-associated plastic flow rule with a suitable plastic function (Q^p). For the sake of simplicity, the confining pressure-sensitive Drucker-Prager model was used to describe the plastic behavior, whereas the plastic loading function has been modified to consider the effect of damage in plasticity (Zhang & Cai, 2001).

$$F^P = F\left(\sigma_{ij}, L\right) = \alpha\sigma_m + \sqrt{J_2^{'}} - e^{-L}C \tag{25}$$

$$Q^p = F\left(\sigma_{ij}\right) = \beta\sigma_m + \sqrt{J_2^{'}} \tag{26}$$

$$\sigma_m = \frac{\sigma_{kk}}{3},\ J_2^{'} = s_{ij}s_{ij}$$

Where, σ_{kk} denotes the first invariant of the 'nominal' stress tensor (σ_{ij}), J_2' the second invariant of the deviatoric stress tensor (s_{ij}), α friction, C cohesion and β the dilation parameter. Traditionally the effective stress tensor has been usually used in the plastic yield function rather than nominal stress to take into account the damage effect on rock plastic behavior. In equivalence, the cohesion parameter can be multiplied by expression e^{-L} (Salari et.al. 2004). The two Drucker-Prager parameters α and C may be expressed in terms of the uniaxial tensile (f_t) and compressive strength (f_c) values as

$$\alpha = 3\sqrt{\frac{2}{3}}\left(\frac{f_c - f_t}{f_c + f_t}\right) \text{ and } C = 2\sqrt{\frac{2}{3}}\left(\frac{f_c \cdot f_t}{f_c + f_t}\right) \tag{27}$$

Adopting a non-associated flow rule

$$\dot{\varepsilon}_{ij}^{p} = \dot{\lambda}^{p} \frac{\partial Q^{p}}{\partial \sigma_{ij}} \tag{28}$$

Here $\dot{\varepsilon}_{ij}^{p}$ is the rate of plastic strain tensor and $\dot{\lambda}^{p}$ is the plastic multiplier. In addition, $\dot{\lambda}^{p}$ is a non-negative scalar expressed from the loading-unloading condition according to the Kuhn-Tucker relations:

$$F^{P} = F\left(\sigma_{ij}, L\right) = 0,\ \dot{\lambda}^{p} \geq 0,\ F^{P}\ \dot{\lambda}^{p} = 0 \tag{29}$$

In the absence of logarithmic damage evolution ($\dot{L} = 0$), the plastic multiplier is determined from the plastic consistency condition ($\dot{F}^{p} = 0$) as below

$$\dot{\lambda}^{p} = \frac{\dfrac{\partial F^{p}}{\partial \sigma_{ij}} E_{ijkl} \dot{\varepsilon}_{kl}}{\dfrac{\partial F^{p}}{\partial \sigma_{ij}} E_{ijkl} \dfrac{\partial Q^{p}}{\partial \sigma_{kl}}} \tag{30}$$

The rate form of constitutive equations (9) in elastic-plastic condition without logarithmic damage evolution ($\dot{L} = 0$) can be expressed

$$\dot{\sigma}_{ij} = E_{ijkl}^{t^{ep}} \dot{\varepsilon}_{kl} \tag{31}$$

In the above equation, $E_{ijkl}^{t^{ep}}$ is the tangent elastic stiffness tensor in the elastic-plastic condition. Substitution the increment of plastic strain tensor in equation (28) into equation (9) without logarithmic damage evolution, leads to

$$E_{ijkl}^{t^{ep}} = E_{ijkl} - \frac{\left(E_{ijqs} \dfrac{\partial F^{p}}{\partial \sigma_{qs}}\right) \otimes \left(E_{klcd} \dfrac{\partial Q^{p}}{\partial \sigma_{cd}}\right)}{\left(\dfrac{\partial F^{p}}{\partial \sigma_{ij}} E_{ijkl} \dfrac{\partial Q^{p}}{\partial \sigma_{kl}}\right)} \tag{32}$$

2.3. Coupled elastoplastic damage behavior

Generally, the plastic flow and damage evolution occur in a coupled process. Due to effect of plasticity and damage process on each other, the plastic and logarithmic damage multipliers should be determined simultaneously. Applying the plastic and damage consistency conditions leads to a coupled system of equations as

$$\begin{cases} \dot{F}^{L}\left(Y_{L}, L\right) = \dfrac{\partial F^{L}}{\partial Y_{L}} \left(\dfrac{\partial Y_{L}}{\partial \varepsilon_{ij}^{e}} \dot{\varepsilon}_{ij}^{e} + \dfrac{\partial Y_{L}}{\partial L} \dot{L}\right) - \dfrac{\partial r\left(L\right)}{\partial L} \dot{L} = 0 \\ \dot{F}^{p}\left(\sigma_{ij}, L\right) = \dfrac{\partial F^{P}}{\partial \sigma_{ij}} \dot{\sigma}_{ij} + \dfrac{\partial F^{p}}{\partial L} \dot{L} = 0 \end{cases} \tag{33}$$

Substitution of the equations (9) & (12) into system of equations (33), a system of equations in matrix form can be expressed

$$\begin{bmatrix} \left(\frac{\partial r(L)}{\partial L}-\frac{\partial Y_L}{\partial L}\right) & \left(\frac{\partial Y_L}{\partial \varepsilon_{ij}^e}\frac{\partial Q^p}{\partial \sigma_{ij}}\right) \\ \left(\frac{\partial F^p}{\partial \sigma_{ij}}E_{ijkl}\varepsilon_{kl}^e-\frac{\partial F^P}{\partial L}\right) & \left(\frac{\partial F^p}{\partial \sigma_{ij}}E_{ijkl}\frac{\partial Q^p}{\partial \sigma_{kl}}\right) \end{bmatrix}\begin{bmatrix} \dot{L} \\ \dot{\lambda}^p \end{bmatrix}=\begin{bmatrix} \frac{\partial Y_L}{\partial \varepsilon_{ij}^e}\dot{\varepsilon}_{ij} \\ \frac{\partial F^p}{\partial \sigma_{ij}}E_{ijkl}\dot{\varepsilon}_{kl} \end{bmatrix} \tag{34}$$

The plastic and logarithmic damage multipliers were calculated based on the Cramer's Rule to solve the system of equations as following

$$\dot{L}=\frac{\left(\frac{\partial F^p}{\partial \sigma_{ij}}E_{ijkl}\frac{\partial Q^p}{\partial \sigma_{kl}}\right)\left(\frac{\partial Y_L}{\partial \varepsilon_{ij}^e}\dot{\varepsilon}_{ij}\right)-\left(\frac{\partial Y_L\partial Q^p}{\partial \varepsilon_{ij}^e\partial \sigma_{ij}}\right)\left(\frac{\partial F^p}{\partial \sigma_{ij}}E_{ijkl}\dot{\varepsilon}_{kl}\right)}{\left(\frac{\partial r(L)}{\partial L}-\frac{\partial Y_L}{\partial L}\right)\left(\frac{\partial F^p}{\partial \sigma_{ij}}E_{ijkl}\frac{\partial Q^p}{\partial \sigma_{kl}}\right)-\left(\frac{\partial Y_L\partial Q^p}{\partial \varepsilon_{ij}^e\partial \sigma_{ij}}\right)\left(\frac{\partial F^p}{\partial \sigma_{ij}}E_{ijkl}\varepsilon_{kl}^e-\frac{\partial F^p}{\partial L}\right)} \tag{35}$$

$$\dot{\lambda}^P=\frac{\left(\frac{\partial r(L)}{\partial L}-\frac{\partial Y_L}{\partial L}\right)\left(\frac{\partial F^p}{\partial \sigma_{ij}}E_{ijkl}\dot{\varepsilon}_{kl}\right)-\left(\frac{\partial F^p}{\partial \sigma_{ij}}E_{ijkl}\varepsilon_{kl}^e-\frac{\partial F^p}{\partial L}\right)\left(\frac{\partial Y_L}{\partial \varepsilon_{ij}^e}\dot{\varepsilon}_{ij}\right)}{\left(\frac{\partial r(L)}{\partial L}-\frac{\partial Y_L}{\partial L}\right)\left(\frac{\partial F^p}{\partial \sigma_{ij}}E_{ijkl}\frac{\partial Q^P}{\partial \sigma_{kl}}\right)-\left(\frac{\partial Y_L\partial Q^P}{\partial \varepsilon_{ij}^e\partial \sigma_{ij}}\right)\left(\frac{\partial F^P}{\partial \sigma_{ij}}E_{ijkl}\varepsilon_{kl}^e-\frac{\partial F^P}{\partial L}\right)} \tag{36}$$

3. The model algorithm

The classic step by step iterative approach including elastic prediction, plastic and damage corrections was implemented to the numerical computation procedure according to the elastoplastic-logarithmic damage model. With assuming the increment of total strain at each step, the increments of stress, plastic strains and logarithmic damage variable are calculated in each element and added to their previous values based on the constitutive equation in rate form. The nth step of the numerical computational procedure can be described as following:

1) The tensors $\sigma_{ij}^{(n-1)}$, $\varepsilon_{ij}^{(n-1)}$, $\varepsilon_{ij}^{e(n-1)}$, $\varepsilon_{ij}^{p(n-1)}$ and the logarithmic damage variable $L^{(n-1)}$ have been determined at the end of previous step $(n-1)$.
2) Assuming an increment of total strain $(\Delta\varepsilon_{ij}^{(n)})$, the total strain tensor can be calculated as

$$\varepsilon_{ij}^{(n)}=\varepsilon_{ij}^{(n-1)}+\Delta\varepsilon_{ij}^{(n)} \tag{37}$$

3) The elastic behavior without plasticity and damage is assumed as trial elastic prediction

$$\tilde{\varepsilon}_{ij}^{e(n)}=\varepsilon_{ij}^{(n)}-\varepsilon_{ij}^{P(n-1)},\ \tilde{\sigma}_{ij}^{e(n)}=\sigma_{ij}^{(n-1)}+e^{-L^{(n-1)}}E_{ijkl}^0\Delta\varepsilon_{kl}^{(n)} \tag{38}$$

4) The logarithmic damage criterion $F^L(Y_L, L)$ in equation (19) and plastic yield function $F^P(\sigma_{ij}, L)$ in equation (25) are calculated and checked.
5) If $F^L \geq 0$ & $F^P < 0$ only damage evolution occurs in absence of plasticity. The increment of logarithmic damage variable is calculated from equation (21), and then the logarithmic damage variable is updated as $L^{(n)} = L^{(n-1)} + \dot{L}^{(n)}$.
6) If $F^P \geq 0$ & $F^L < 0$ only plastic flow occurs in absence of damage evolution. The plastic multiplier is computed according to equation (30). The increment of plastic strain tensor is calculated at nth step as following. Then the plastic strain tensor is updated.

$$\dot{\varepsilon}_{ij}^{p} = \dot{\lambda}^{P} \frac{\partial Q^{P}}{\partial \sigma_{ij}^{(n)}} = \dot{\lambda}^{P} \left(\frac{1}{3} \beta \delta_{ij} + \frac{s_{ij}^{(n)}}{\sqrt{J_2^{/(n)}}} \right) \tag{39}$$

Based on equation (9), the stress tensor is corrected as following

$$\sigma_{ij}^{(n)} = \tilde{\sigma}_{ij}^{(n)} - e^{-L^{(n-1)}} E_{ijkl}^{0} \dot{\varepsilon}_{kl}^{p^{(n)}} \tag{40}$$

7) If $F^P \geq 0$ & $F^L \geq 0$, the plastic flow and damage evolution occur simultaneously. The plastic and damage multipliers are computed based on equations (35) & (36). The increment of plastic strain tensor is calculated from equation (39), and the logarithmic damage variable is updated at nth step. Finally based on equation (9), the stress tensor is corrected as following

$$\sigma_{ij}^{(n)} = \tilde{\sigma}_{ij}^{(n)} - e^{-L^{(n-1)}} E_{ijkl}^{0} \left(\dot{\varepsilon}_{kl}^{p^{(n)}} + \dot{L} \tilde{\varepsilon}_{kl}^{e(n)} \right) \tag{41}$$

4. The developed model input parameters

For analysis of problems, the physical, mechanical and strength properties of constitutive model are considered as essential input parameters. Therefore, to use a constitutive model, the cognition of its input parameters is necessary. On the other hand, the simplicity and accuracy of determining the input parameters of the constitutive model is important. Hence, the input parameters of the elastoplastic-logarithmic damage model consist of three parts:

1) Elastic parameters: Including Young's modulus (E^0) and Poisson's ratio (v^0),
2) Plastic parameters: Including Cohesion (C), friction (α) and dilation (β) parameters,
3) Damage parameters: Including Strain energy corresponding to the maximum strength (r_0) and Fracture energy per unit volume (g_f).

5. Analytical solution of the coupled elastoplastic logarithmic damage model

In this section, the behavior of rock sample under uniaxial tensile strength test (UTS) condition has been investigated by closed form solution method. In this test, the maximum principal

stress (σ_1) is in the direction of the positive y axis ($\sigma_1 = \sigma_{yy} \geq 0$), while all other stress components equal to zero. As previously mentioned, the logarithmic damage criterion in UTS test can be written as below:

$$F^{+L}\left(Y_L, L\right) = \frac{1}{2} e^{-L} \varepsilon_i E^0 \varepsilon_i - r_{0t} e^{-K_t L} \tag{42}$$

According to the above equation, the thermodynamic force associated with logarithmic damage is written as follow:

$$Y_L = \frac{1}{2} e^{-L} \varepsilon_i E^0 \varepsilon_i \Rightarrow Y_L = \frac{1}{2} \sigma_i \varepsilon_i \tag{43}$$

Due to the fact that the loading is in y direction, the equation (42) can be written as below:

$$F^{+L}\left(Y_L, L\right) = \frac{1}{2} \sigma_y \varepsilon_y - r_{0t} e^{-K_t L} \tag{44}$$

During the loading, no damage evolution will occur when the damage criterion is negative ($F^{+L} < 0$). Assuming zero initial damage ($L^0 = 0$), the loading process will be continuing until damage criterion turns from negative value to zero ($F^{+L} = 0$). In fact, this moment of loading represents the peak strength in stress-strain curve. Therefore, in this moment, the elastic strain energy corresponding to the maximum uniaxial tensile strength test (r_{0t}) will be determined as follows:

$$F^{+L}\left(Y_L, L\right) = 0 \Rightarrow \frac{1}{2} \sigma_t \varepsilon_t - r_{0t} e^{-K_t L} = 0 \Rightarrow r_{0t} = \frac{\sigma_t^2}{2E^0} \tag{45}$$

By continuing the process of loading, the damage criterion turns from zero to positive value ($F^{+L} > 0$). Therefore, at this moment of loading, damage evolution will occur ($\dot{L} \neq 0$). In this regard, by substitution equation (45) into (42), the damage criterion is written as follow:

$$F^{+L}\left(Y_L, L\right) = \frac{1}{2} e^{-L} \varepsilon_y E^0 \varepsilon_y - \frac{\sigma_t^2}{2E^0} e^{-K_t L} = 0 \tag{46}$$

According to the above equation, the exponential variable (e^{-L}) can be written as follow:

$$e^{-L} = \left(\frac{\varepsilon_y}{\varepsilon_t}\right)^{\frac{-2}{1-K_t}} \tag{47}$$

By substitution equation (47) into stress-strain equation, the relationship between stress and strain is calculated as follow:

$$\sigma_y = e^{-L} E^0 \varepsilon_y \ , \sigma_t = E^0 \varepsilon_t \Rightarrow \frac{\sigma_y}{\sigma_t} = e^{-L} \frac{\varepsilon_y}{\varepsilon_t} \Rightarrow \sigma_y = \sigma_t \left(\frac{\varepsilon_y}{\varepsilon_t}\right)^{-\frac{1+K_t}{1-K_t}} \tag{48}$$

Finally, by reversing the above equation, the elastic-damage strain (ε_y^{ed}) is determined as below:

$$\varepsilon_y^{ed} = \varepsilon_t \left(\frac{\sigma_y}{\sigma_t} \right)^{-\frac{1-K_t}{1+K_t}} \tag{49}$$

On the other hand, in this paper, the Drucker-Prager yield criterion has been employed to calculate the irreversible strains. In this regard, according to equation (25), the plastic yield function can be written as follow:

$$F^P = \alpha \sigma_m + \sqrt{J_2^{'}} - e^{-L} C \tag{50}$$

According to equation (25), in UTS test:

$$\sigma_m = \frac{\sigma_y}{3},\ J_2^{'} = \frac{2}{3}\sigma_y^2 \Rightarrow F^P = \alpha \frac{\sigma_y}{3} + \sqrt{\frac{2}{3}}\sigma_y - e^{-L} C \tag{51}$$

Similar to the damage mode, at the initial stage of loading, the value of plastic yield criterion (equation (50)) is negative ($F^P < 0$). Therefore, no plastic flow occur. By increasing the loading, the value of plastic yield function turns from negative to zero in a certain stress value ($F^P = 0$). In the presence of plastic flow and absence of damage evolution, according to the equation (51), the plastic yield stress can be determined as below:

$$F^p = \frac{1}{3}\alpha \sigma_y + \sqrt{\frac{2}{3}}\sigma_y - e^{-L} C = 0,\ L^0 = 0 \Rightarrow \sigma_{yield} = \left(\frac{C}{\frac{\alpha}{3} + \sqrt{\frac{2}{3}}} \right) \tag{52}$$

By continuing the process of loading, after the strain corresponding to tensile strength (ε_t), in addition to plastic flow, the damage evolution will occur simultaneously. Therefore, the plastic yield function has a softening behavior. In this regard, by substitution equation (49) into (51), the relationship between stress and strain can be written as below:

$$F^p = 0 \Rightarrow \sigma_y = \left(\frac{C}{\frac{\alpha}{3} + \sqrt{\frac{2}{3}}} \right) \left(\frac{\varepsilon_y}{\varepsilon_t} \right)^{\frac{-2}{1-K_t}} \varepsilon_y > \varepsilon_t \tag{53}$$

Finally, by reversing the above equation, the elastoplastic strain (ε^{ep}) is determined as below:

$$\varepsilon_y^{ep} = \varepsilon_t \left(\left[\frac{\sqrt{\frac{2}{3}} - \frac{\alpha}{3}}{C} \right] \sigma_y \right)^{-\frac{1-K_t}{2}} \tag{54}$$

According to equations (51) and (54), the complete stress-strain curve based on elastoplastic-logarithmic damage model can be drawn. The Fig. 2 shows the complete stress-strain curve for Oolitic limestone in UTS test condition based on the analytical solution using input parameters in Table 1. In this figure, the violet and red lines represent elastic-damage and elastoplastic curves respectively.

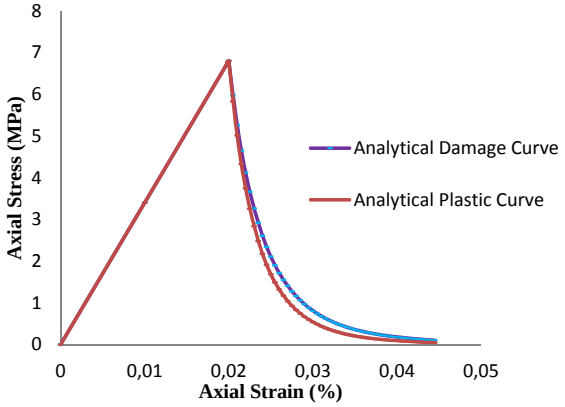

Fig. 2. The complete stress-strain curves based on elastic-damage and elastoplastic models

In this step, the main purpose is to combine the separate stress-strain curves based on elastoplastic and elastic-damage models and to calculate the united stress-strain curve based on coupled elastoplastic-logarithmic damage model by analytical method.

According to Fig. 3, in the first stage, an arbitrary level of stress was determined on the figure (K). Now, from this level of stress, a line parallel to the strain axis was drawn. The intersection of this line with the stress-strain curves corresponding to elastoplastic and elastic-damage models have been called B and C respectively.

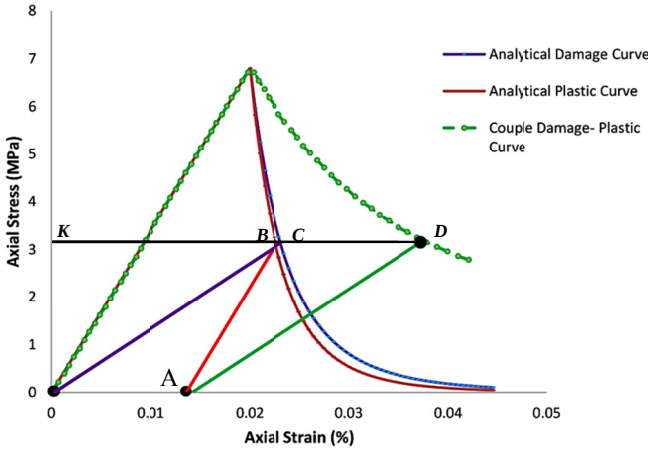

Fig. 3. The combined stress-strain curve based on the coupled elastoplastic damage model

In the second stage, based on the theory of plasticity, due to the lack of stiffness degradation, the slope of unloading (red) line is parallel to the initial elastic modulus. The intersection of this line with strain axis has been called A. In fact, OA represents the irreversible strain.

In the third stage, based on the theory of damage, due to the lack of irreversible strain in elastic-damage stress-strain curve, the unloading (violet) line returns to origin point (O). Finally, to obtain the combined stress- strain curve corresponding to the coupled elastoplastic-damage model, a green line was drawn parallel to the violet line from the point A. The intersection of this green line and arbitrary stress level (black line) has been called point D which has been located on the combined stress-strain curve based on the coupled elastoplastic-logarithmic damage model.

By repeating the above steps at different stress levels, all points of the stress-strain curve based on the coupled elastoplastic damage were obtained. Accordingly, the stress-strain relation based on the coupled elastoplastic logarithmic damage model in post peak region can be calculated as follows:

$$\varepsilon_{yy} = \varepsilon_{yy}^{ed} + \varepsilon_{yy}^{ep} - \left(\frac{\sigma_{yy}}{E^0}\right) \tag{55}$$

Finally, by substitution equations (51) and (54) into (55), the above equation can be written as below:

$$\varepsilon_{yy} = \varepsilon_t \left(\frac{\sigma_y}{\sigma_t}\right)^{-\frac{1-K_t}{1+K_t}} + \varepsilon_t \left(\left[\frac{\sqrt{\frac{2}{3}} - \frac{\alpha}{3}}{C}\right]\sigma_y\right)^{-\frac{1-K_t}{2}} - \left(\frac{\sigma_{yy}}{E^0}\right) \tag{56}$$

6. Numerical simulation with the proposed constitutive model

In this investigation, to simulate the behavior of rock, the coupled elastoplastic-logarithmic damage model programmed and implemented in a commercial software environment. Similar to all of the constitutive models, in this developed model, the new stress tensor is calculated based on applied incremental strain tensor.

Generally, to investigate the softening behavior of rocks on post peak region, the complete stress-strain curve obtained by servo control test machine is necessary. In this regard, the area under this curve represents the fracture energy per unit volume (g_c) of rocks. In addition, the shape of stress-strain curve especially after maximum point represents the mechanism of fracture and brittleness of rocks. In this section, in order to numerical simulation under various loading conditions, the behavior of an Oolitic limestone with UCS and UTS equal to 68 MPa and 6.8 MPa respectively reported by Brady & Brown, 2005 has been selected as a basis of modeling. The complete stress-strain curve of the Oolitic limestone within unloading and reloading cycles (stiffness degradation) and plastic strains has been shown in Fig. 4.

In this regard, in the table 1, the parameters of Oolitic limestone reported in Brady & Brown, 2005 have been provided as input data for numerical simulation based on the developed model.

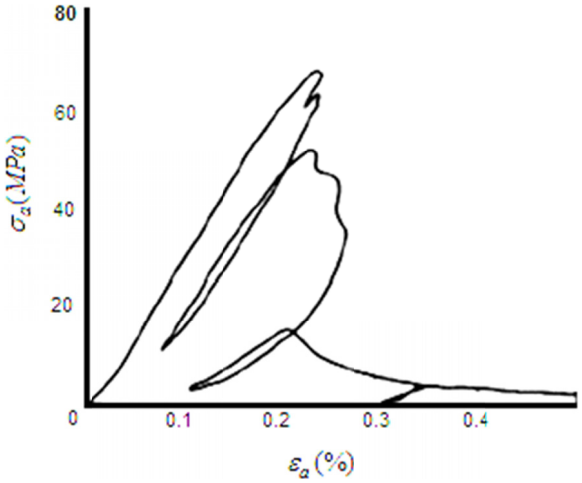

Fig. 4. The complete stress-strain curve of Oolitic limestone (Brady & Brown, 2005)

TABLE 1

Rock properties used in the numerical analysis (Brady & Brown, 2005)

Elastic parameters	Plastic parameters	Damage parameters
$E^0 = 34$ GPa $v^0 = 0.3$	$C = 5$ MPa $\alpha = 0.4724$ $\beta = 0.4724$	$g_{fcnum} = 110$ MPa $g_{ftnum} = 7$ MPa

According to table 1, there are 7 material parameters needed to calibrate the elastic, plastic and damage behavior. Representative values for the tested Oolitic limestone have been used in the numerical simulation. It should be noted that, in this article, to simulate the behavior of rock according to the proposed model, a rate of velocity equal to 0.2 mm per second has been applied at the top of an element in vertical direction.

6.1. Uniaxial compressive strength test (UCS)

The complete stress-strain curve simulated under uniaxial compressive strength test conditions based on the elastic-logarithmic damage constitutive model without plastic flow is shown in Fig. 5.

As shown in Fig. 5 on post-peak region, the strain softening behavior and stiffness degradation resulting from damage occur during the cycles of unloading and reloading without any plastic strain. To show the actual behavior of rocks, in addition to the damage evolution, simulation of the plastic deformation which occur under loading and unloading conditions is essential. Hence the complete stress-strain curve of Oolitic limestone simulated with the coupled elastoplastic-logarithmic damage model under UCS test conditions has been illustrated in Fig. 6.

According to Fig. 6, if the developed coupled elastoplastic-logarithmic damage model has been employed instead of only damage model, the irreversible strains due to the plastic flow can be simulated in addition to the stiffness degradation and softening behavior.

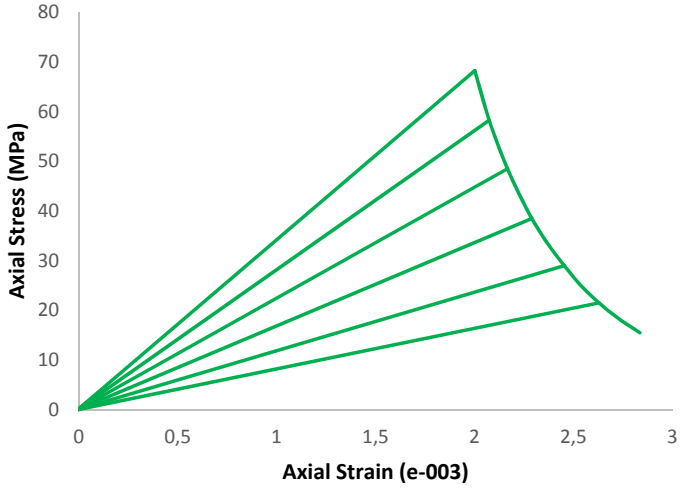

Fig. 5. The complete stress-strain curve simulated based on the elastic-logarithmic damage model without plastic flow

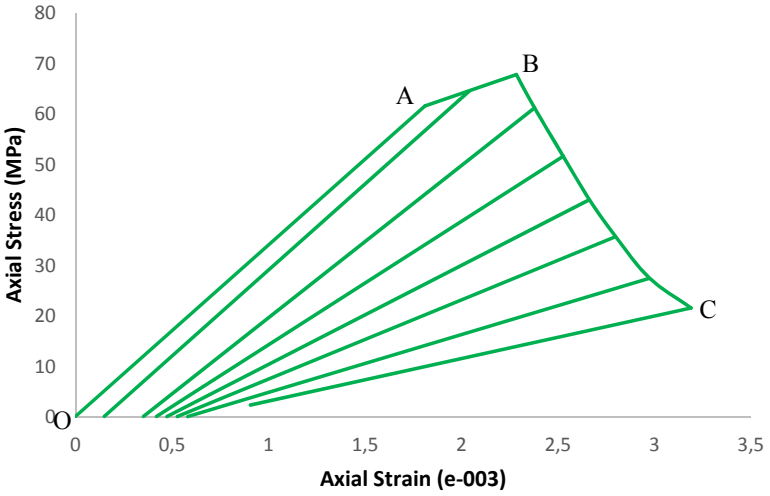

Fig. 6. The complete stress-strain curve of Oolitic limestone simulated with the coupled elastoplastic-logarithmic damage model

According to the simulation results, three distinctive regions can be observed. In the first phase OA, the material behavior remains linear elastic. Hence neither plastic flow nor damage evolution occur in this phase. The slopes of the axial stress-strain curves are the same as the Young modulus. As can be seen in the Fig. 6, after the yield stress (point A), the behavior of Oolitic limestone changes from elastic to plastic hardening immediately. The phase AB corresponds to hardening behavior prior to peak strength as a result of plasticity. This process continues until the maximum point (peak strength). In the third phase BC, the damage evolution law also is activated.

In other words, after this point (B), in addition to softening behavior, according to the cycles of unloading and reloading, the plastic flow and stiffness degradation occur simultaneously. Finally, softening behavior, stiffness degradation and irreversible strains after peak strength because of simultaneous plastic flow and damage evolution can be seen in Fig. 6.Correspondingly, the yield stress (point A) and peak strength (point B) on the stress-strain curve represent the plastic yield surface and damage resistance respectively.

In Fig. 7, to validate the developed model, the complete stress-strain curves for Oolitic limestone based on experimental data and numerical simulation have been illustrated side by side.

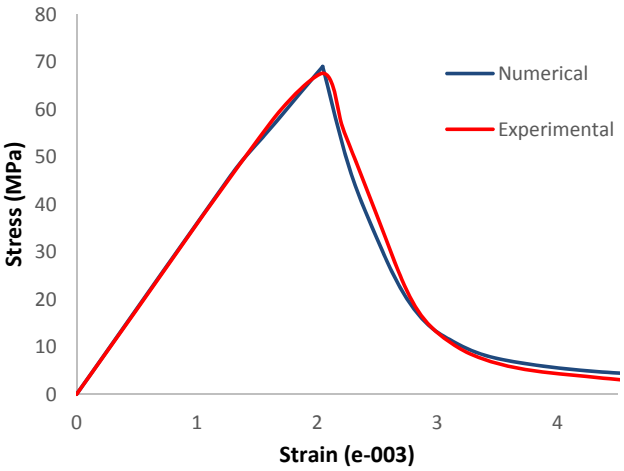

Fig. 7. The complete stress-strain curves corresponding to numerical simulation and experimental data for Oolitic limestone

It can be observed in Fig. 7 that the mechanical responses simulated with the developed coupled elastoplastic-logarithmic damage model are in agreement with the experimental Oolitic limestone behavior consisting of initial linear elastic, hardening before peak strength and finally softening after peak strength.

According to Fig. 7, in addition to comparing the complete stress-strain curves corresponding to experimental data (red line) and numerical simulation (blue line), we can have a good judge about the developed model. In this regard, the initial portions of the curves including elastic and plastic hardening phases are substantially consistent. On the other hand, the plastic yield surface and damage resistance on the both curves are matched together. The softening behavior of rock sample is evident on the post peak region for two curves. In other words, according to Fig. 7, it can be concluded that the developed model is predominantly acceptable.

6.2. Uniaxial tensile strength test (UTS)

Fig. 8 illustrates the simulated complete stress-strain curve of Oolitic limestone in uniaxial tensile strength conditions by implementing the developed elastoplastic-logarithmic damage model.

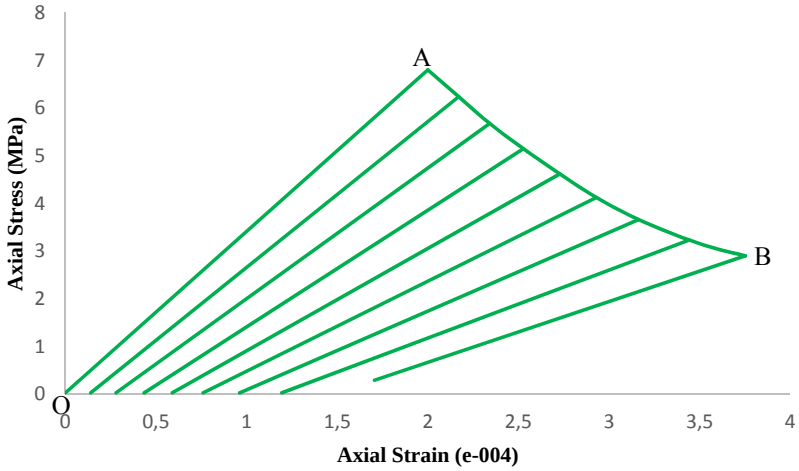

Fig. 8. The stress-strain curve under UTS condition based on the developed coupled elastoplastic logarithmic damage model

According to the Fig. 8, the simulated irreversible strains and stiffness degradation based on the developed coupled elastoplastic-logarithmic damage model within softening behavior is evident. Due to the low tensile strength compared to the compressive strength, the plastic hardening phase does not occur in this test. In other words, before reaching the plastic yield surface, the damage process occurs. Therefore, in this test, instead of three distinctive phases, two phases are observed. Initially the material behaves linearly elastically until the plastic dilatation reaches a critical limit defined by the damage resistance (point B) of the material, and the damage process is mobilized resulting in large deterioration of strength down to a residual strength level as well as in progressive damage of the elastic stiffness in the softening regime. In other words, on the second phase AB, in addition to softening behavior, the plastic flow and damage evolution occur simultaneously.

6.3. Triaxial compressive strength test

One of the observed mechanisms reported by different researchers concerns the behavior of rocks under triaxial loading conditions and its dependency on the confining pressure. According to Fig. 9, with increasing confining pressure the rock strength and ductility increase too (Brady & Brown, 2005).

In this section, the main objective of the simulation of triaxial compressive strength test is to investigate the dependency of the strength and ductility on confining pressure. Accordingly, the Oolitic limestone was modeled under triaxial compressive loading conditions based on the developed coupled elastoplastic-logarithmic damage model. For this purpose, the confining pressures equal to 3 and 6 MPa were applied on both sides of the sample. As a result of applying confining pressure, the peak strength of rock changes from 68 MPa to 75 MPa and 84 MPa respectively as shown in Fig. 10.

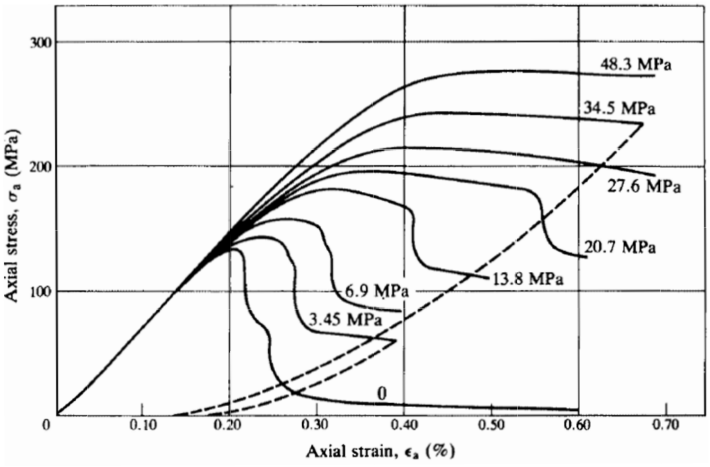

Fig. 9. Complete stress-strain curves obtained in triaxial compressive tests on Tennessee Marble at the confining pressures indicated by the numbers on the curves (Brady & Brown, 2005)

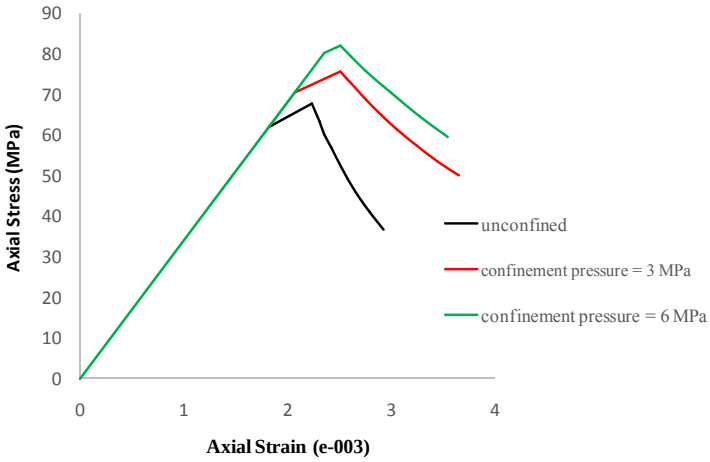

Fig. 10. The simulated increase of strength and ductility based on the coupled elastoplastic-logarithmic damage model

6.4. Investigation of the rock brittleness based on the proposed model

To determine the brittleness and ductility of the rock based on the proposed constitutive model, the parameter $K = \frac{r_0}{g_f}$ can be used as a controlling parameter. So that, by increasing the value of the controlling parameter, the brittleness increases, and consequently the ductility decreases. In this section, assuming constant parameter r_0 (the elastic strain energy corresponding to the uniaxial compressive strength), the effect of variations of parameter g_f (fracture energy

per unit volume or area under the complete stress-strain curve) on the complete stress-strain curve has been investigated.

In Fig. 11, the effects of increasing parameter g_f on the complete stress-strain curve in the uniaxial compressive strength test (UCS) for Oolitic limestone is shown.

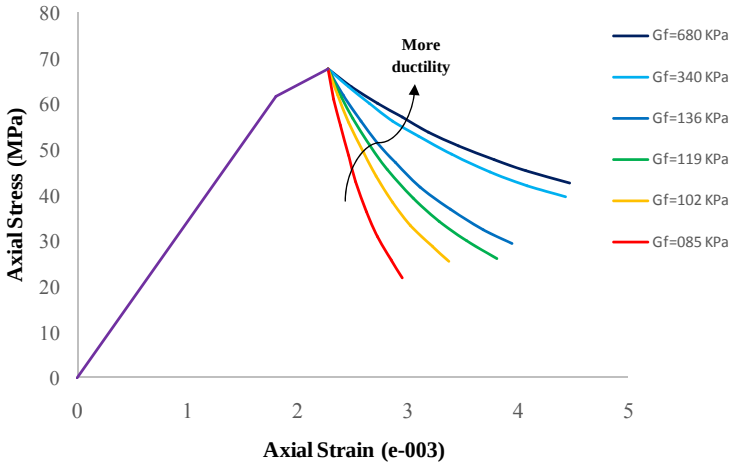

Fig. 11. The complete stress-strain curve based on the variations of parameter g_f.

According to Fig. 11, while parameter r_0 is equal to 68 KPa, the parameter g_f varies from 85 KPa to 680 KPa to investigate the effect of this parameter on rock ductility based on the coupled elastoplastic-logarithmic damage model. Accordingly, with increasing parameter g_f the behavior of rock changes from brittle to ductile gradually, for the area under the complete stress-strain curve increases.

7. Conclusion

The proposed coupled elastoplastic-logarithmic damage model has been formulated within the framework of the principles and laws of irreversible thermodynamics. In the developed model, it is assumed that no damage evolution and stiffness degradation will occur prior to the maximum strength (pre peak). In other words, the strain energy applied by the loading is stored in these type of materials as much as possible. Finally, due to sudden release of this energy, rock is immediately fractured. In addition to the small number of input parameters, the simplicity in the determination of them is another characteristic of the proposed model. In this regard, all parameters used in the proposed model are calculated by standard experiments. Using the logarithmic variable damage, the thermodynamic force associated with damage gets a certain physical meaning.

Finally, the experimental Oolitic limestone rock behavior was simulated based on the developed model. The numerical simulation results based on the coupled elastoplastic-logarithmic damage model in experimental scale shows both irreversible strain resulting from plastic flow, stiffness degradation due to damage evolution and softening. Furthermore, the confinement pressure dependency of rock behavior was simulated in according to experimental observations.

Reference

Addessi D., Marfia S., Sacco., E. 2002. *A Plastic Nonlocal Damage Model*. Computer Methods in Applied Mechanics and Engineering 191 (13-14), 1291-1310.

Bazant Z.P., Kim S.S., 1979. *Plastic-Fracturing Theory for Concrete*. ASCE Journal of Engineering Mechanics 105 (3), 407-421.

Brady B.H.G., Brown E.T., 2005. *Rock Mechanics for underground mining*. Springer Science.

Carol I., Rizzi E., Willam K., 2001. *On the formulation of anisotropic elastic degradation. I. Theory based on a pseudo--logarithmic damage*. International Journal of Solids and Structures 38: 491-518.

Chiarellia A.S., Shao J.F., Hoteit N., 2003. *Modeling of elastoplastic damage behavior of a claystone*. International Journal of Plasticity 19, 23-45

Conil N., Djeran-Maigre I., Cabrillac R., Su K., 2004. *Thermodynamics modelling of plasticity and damage of argillite*. C. R. Mecaniqu 332; 841-848.

Dragon A., Morz Z., 1979. *A Continuum Theory for Plastic-Brittle Behavior of Rock and Concrete*. International Journal of Engineering Scienc 17 (2), 121-137.

Hansen E., Willam K., Carol I., 2001. *A Two-Surface Anisotropic Damage/Plasticity Model for Plain Concrete*, in Fracture Mechanics of Concrete Materials, de Borst, R. (Ed.), A.A. Balkema, Rotterdam, 549-556.

Jefferson A.D., 2003. *Craft – A Plastic-Damage-Contact Model for Concrete. I. Model Theory and Thermodynamic Considerations*. International Journal of Solids and Structure 40 (22), 5973-5999.

Kamal B., Thapa, Yazdani S., 2013. *Combined damage and plasticity approach for modeling brittle materials with application to concrete*. International Journal of Civil And Structural Engineering 3, 513-525.

Lemaitre J., Desmorat R., 2005. *Engineering Damage Mechanics*. Springer-Verlag Berlin Heidelberg.

Li Y., Zhu W., Fu J., Guo Y., Qi Y., 2014. *A damage rheology model applied to analysis of splitting failure in underground caverns of Jinping I hydropower station*. International Journal of Rock Mechanics and Mining Sciences 71.

Molladavoodi H., 2015. *Sliding and damage criteria investigation of a micromechanical damage model for closed frictional microcracks*. Computers and Geotechnics 67, 135-141.

Molladavoodi H., Mortazavi A., 2011. *A damage-based numerical analysis of brittle rocks failure mechanism*. Finite Elements in Analysis and Design 9, 911-1003.

Mortazavi A., Molladavoodi H., 2012. *A numerical investigation of brittle rock damage model in deep underground openings*. Engineering Fracture Mechanics 90, 101-120.

Ortiz M., 1985. *A Constitutive Theory for the Inelastic Behavior of Concrete*. Mechanics of materials 4 (1), 67-93.

Ortiz M., Popov E.P., A., 1982. *Physical Model for the Inelasticity of Concrete*. Proceedings of Royal Society of London A383, 101-125.

Rashid K., Abu Al-Rub, George Z. Voyiadjis. 2003. *On the coupling of anisotropic damage and plasticity models for ductile materials*. International Journal of Solids and Structures 40; 2611-2643.

Salari M.R., Saeb S., Willam K.J., Patchet S.J., Carrasco R.C., 2004. *A Coupled Elastoplastic Damage Model for Geomaterials*. Computer Methods in Applied Mechanics and Engineering 193 (27-29), 2625-2643.

Simo J.C., Ju. J.W., 1987. *Strain-and-Stress-Based Continuum Damage Models – I. Formulation*. International Journal of Solids Structures 23 (7), 821-840.

Shao J.F., Jia Y., Kondo D., Chiarelli A.S., 2006. *A coupled elastoplastic damage model for semi-brittle materials and extension to unsaturated conditions*. Mechanics of Materials 38, 218-232.

Voyiadjis G.Z., Taqieddin Z.N., Kattan P.I., 2008. *Anisotropic Damage-Plasticity Model for Concrete*. International Journal of Plasticity 24 (10), 1946-1965.

Wang H., Li Y., Li S., Zhang Q., Liu J., 2016. *An elasto-plastic damage constitutive model for jointed rock mass with an application*. Geomechanics and Engineering 11 (1).

Yazdani S., Karnawat S., 1996. *A Constitutive Theory for Brittle Solids with Application to Concrete*. International journal of damage mechanics 5 (1), 93-110.

Yazdani S., Schreyer H.L., 1990. *Combined Plasticity and Damage Mechanics Model for Plain Concrete*. ASCE Journal of Engineering Mechanics 116 (7), 1435-1450.

Zhang W., Cai Y., 2001. *Continuum Damage Mechanics and Numerical Applications*. Springer.

Zhu Q.Z., Shao J.F., Kondo D., 2008. *Micromechanical analysis of coupling between anisotropic damage and friction in quasi brittle materials: role of the homogenization scheme*. Int. J. Solids Struct. 45, 1385-405.